Available online at www.sciencedirect.com

SciVerse ScienceDirect

Physics Procedia 35 (2012) 111 – 116

Physics Procedia

Positron Studies of Defects 2011

Development of a Slow Positron Beam System for in-situ Lifetime Measurements during Ion Beam Irradiation

A. Kinomura*, R. Suzuki, T. Ohdaira, N. Oshima, B. E. O'Rourke and T. Nishijima

National Institute of Advanced Industrial Science and Technology (AIST), 1-1-1 Umezono, Tsukuba, Ibaraki 305-8568, Japan

Abstract

A slow-positron beam system for in-situ positron lifetime measurements during ion beam irradiation is currently under development in order to obtain fundamental information on radiation-induced defects. The system uses a high-intensity positron beam generated through pair-creation by a 70 MeV electron beam from a linear accelerator. The system has typical pulsing electrodes for chopping and bunching positrons. The incident directions of positrons and ions are 0° and 45° to the surface normal of samples, respectively. H, He and inert-gas ions up to 150 keV can be introduced to a target chamber with the irradiation temperature variable from room temperature to 600 °C. In a preliminary examination of the beamlines, 150 keV Ar^+, electrons from a photocathode and positrons from a radioisotope were successfully transported to the target chamber from their respective sources. In addition, in-situ lifetime measurements using the existing positron beamline were demonstrated.

Keywords: slow positron; positron lifetime spectroscopy; ion irradiation; in-situ irradiation

1. Introduction

Formation and kinetics of defects induced by energetic particles such as neutrons and ions have been one of the key issues to study radiation damage of nuclear materials or ion implantation for semiconductor devices. Most of the previous studies on radiation-induced defects have been performed ex-situ, implying that the characterization of defects is performed after the introduction of defects using separate experimental equipments. On the other hand, it is conceivable that in-situ characterization techniques, which realize simultaneous analysis and irradiation, can provide us with much more information on defects. Thus, great efforts have been made to develop in-situ characterization techniques to study radiation-induced defects. One initial and still important approach is high-voltage transmission electron microscopy, where electron beams at energies higher than threshold displacement energies of target materials can introduce defects and simultaneously give microscope images during defect formation [1]. An extended approach is a transmission electron microscopy combined with simultaneous ion

* Corresponding author. Tel.: +81-29-861-3243 fax: +81-29-861-5683.
E-mail address: a.kinomura@aist.go.jp.

1875-3892 doi:10.1016/j.phpro.2012.06.020

irradiation equipments [2, 3]. Similarly, ion beam analysis and x-ray diffraction were combined with simultaneous ion irradiation as alternative approaches [4-6]. The benefits of using in-situ characterization techniques are; (1) not to expose samples to air to avoid oxidation, (2) to avoid the introduction of additional defects during sample preparation, (3) to measure samples without changing the irradiation temperature, (4) to monitor time-dependent phenomena and (5) to observe the transient states of defects.

Positron annihilation spectroscopy has been recognized as one of the most advanced defect characterization techniques, as it can detect vacancy-type defects at atomic scales under the detection limits of electron microscopy. An in-situ slow-positron system combined with an ion beam accelerator was developed by Iwai et al. [7]. The Doppler broadening technique was used with slow positrons from a ^{22}Na radioisotope source and defects were introduced by ion beams from a Van-de-Graaff accelerator. This system has been used to investigate time-dependent (i.e., ion-fluence dependent) damage accumulation [7], defect profiles introduced at cryogenic temperatures [8] and transient defect formation during irradiation [9]. To get more direct information on defects, however, positron lifetime spectroscopy combined with ion beam irradiation is desired. Indeed, Tsuchida et al. developed a preliminary positron-lifetime system based on a β^+-γ coincidence method with high-energy positrons from a ^{68}Ge radioisotope source [10]. Since their system didn't use slow positrons, it was difficult to get sufficient depth-resolved information. Therefore, we aim to develop a slow-positron beam system for in-situ lifetime measurements during ion beam irradiation in this study. By using a high-intensity positron beam from an electron linear accelerator, we expect that time-dependent or transient phenomena of defects can be measured with positron lifetime spectroscopy under simultaneous ion irradiation.

2. System overview

In the system of this study, a slow positron beam is generated through electron-positron pair creation using a electron linear accelerator (LINAC). An electron beam is accelerated to ~70 MeV with a pulse width of ~1 μs from the AIST LINAC and the beam is incident on a water-cooled Ta converter with a thickness of 5 mm. The high-energy positrons generated are thermalized on a moderator consisting of 50 μm multicrystalline W foils arranged in a rectangular mesh. The thermalized positrons are extracted by a bias voltage of about 10 V and fed into the positron beamline. An ion beam is generated by an ion accelerator and introduced to the target chamber after mass separation. Figure 1 shows the schematic diagram of the beamlines for electron, positron and ion beams. The positron beam line has 90° bend ducts at 10 points to override or pass through an existing beamline and concrete shield blocks. For transporting positrons, an axial magnetic field of around 50 Gauss is applied to the whole beamline by coils directly connected to vacuum ducts and additional coils for joints such as flanges and valves. A target chamber and a vacuum ducts housing positron-pulsing electrodes were installed in Helmholtz coils with a diameter of ~60 cm. 4 ion pumps and 2 turbo molecular pumps are used for pumping the system including the positron beamline, the target chamber and the ion beamline. The vacuum of the beamlines and the target chamber is maintained in the order of 10^{-5} Pa.

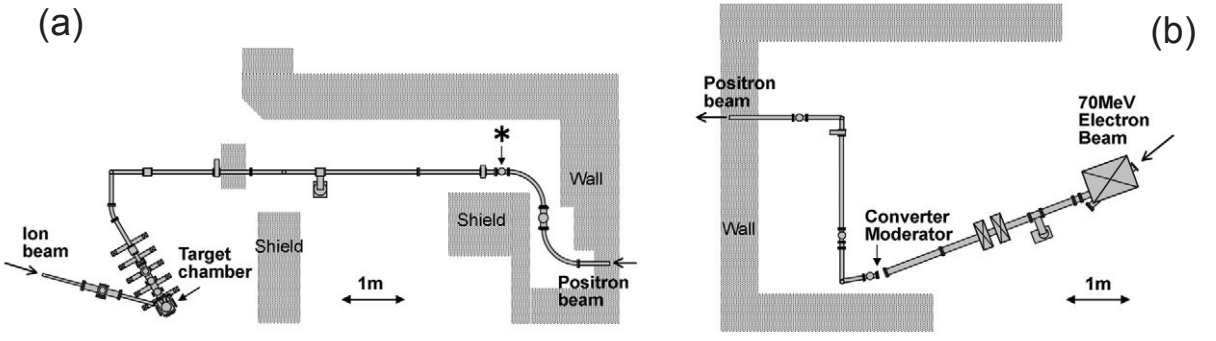

Fig. 1 Plan view of the of the slow-positron beam system for in-situ lifetime measurements during ion beam irradiation. Beamlines in experimental room (a) and the LINAC vault (b). Both beamlines are connected to each other through the wall.

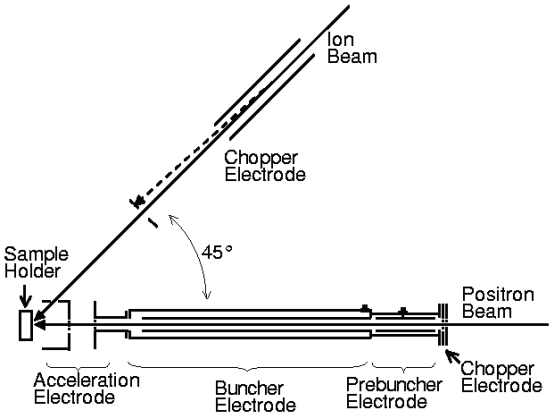

Fig. 2 Schematic diagram of the target chamber and the chopping electrode for positrons and ions.

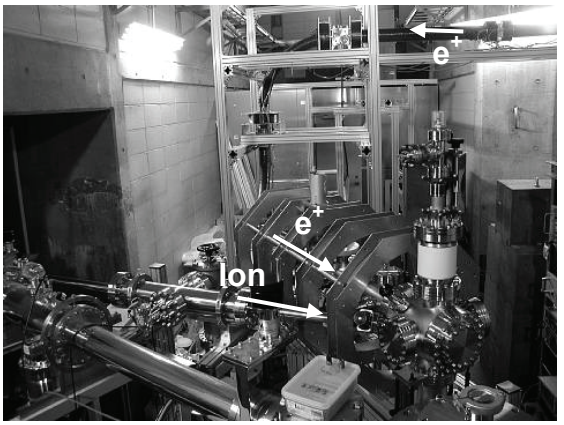

Fig.3 Photograph of the target chamber and the positron and ion beamlines.

Positrons are transported from the W moderator to a chopper electrode which is made of W meshes. The positron pulses are formed by prebuncher and main-buncher electrodes to obtain sufficient pulse width (<200 ps) for positron lifetime measurements. The main-buncher electrode is driven by radio frequency (RF) wave of 165 MHz. The prebuncher and chopper electrode are driven by RF wave of 1/4 of the main-buncher frequency. The sample holder is electrically insulated and can be biased to high voltage which accelerates positrons up to 30 keV. The structure and the function of the positron pulsing electrodes are based on the techniques established in the existing positron beamline at AIST [11].

The incident direction of the ion beam is 45° off the incident direction of the positron beam. The maximum acceleration voltage of the ion accelerator is 150 kV. The ion accelerator has an RF-plasma ion source, where ion species from gas sources such as H_2, He, N_2, Ne and Ar can be accelerated. A typical beam current is 10 μA with a beam diameter of ~1cm. The ion beamline also has a chopper electrode to control the fluence and the time of ion irradiation. A ring electrode after the chopper electrode stops the beam and measures the ion beam current during irradiation. The ion beam is not scanned during irradiation and appropriately defocused on the sample by adjusting lenses at the ion source to achieve nearly uniform irradiation. The sample holder has a graphite heater and thermocouples for sample heating up to 600 °C.

Figure 3 shows a photograph of the target chamber and the incident positron and ion beamlines. The positron beam comes from the upper right-hand side and is fed into the pulsing electrode via the bend ducts. The ion beam comes from the left-hand side and is fed into the target chamber through the gap of the Helmholz coils. As can be seen from Fig. 3, the height of the positron beamline is not constant to override the existing beam line and shield blocks, while the height of the target chamber was adjusted to the height of the ion accelerator.

3. Beam transport test

A 150 keV Ar^+ beam was transported to the target chamber to confirm the alignment of the ion beamline. A glass plate was put on the sample holder. A beam spot was observed as the fluorescence on the glass plate, indicating successful alignment of the beamline and the chamber.

A photocathode-type electron source, which produces a weak electron beam comparable to the expected positron beam, was installed near the position of the converter in the positron beamline. The electrons were extracted with a bias voltage of 10 V and transported along the beamline in the same way as positrons. The transported electrons were detected at the target chamber by a microchannel plate (MCP) and a screen. Figure 4 shows the photograph of the fluorescence induced by transported electrons on the MCP screen. A beam spot can be observed through a window on a conflat flange of 70 mm in diameter. By switching the extraction voltage of the electron source, we confirmed that the observed fluorescence originates from the transported electrons.

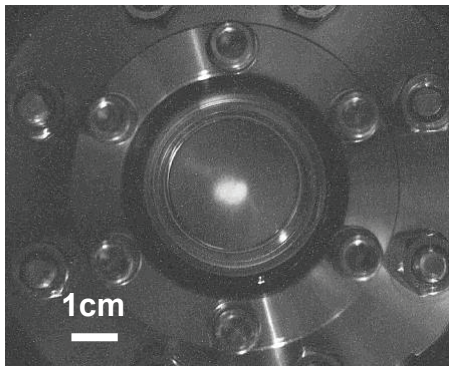

Fig. 4 Fluorescence on the MCP screen showing the electron beam transported through the positron beamline.

A radioisotope (^{22}Na) positron source was installed in the positron beamline at the position denoted by * and an arrow in Fig. 1(a). A W moderator and an extraction electrode were installed together with the ^{22}Na source. The W moderator was annealed at ~2200 °C in vacuum by electron beam heating. Note that the same types of the moderator and the electrode are used at the converter position. The positrons were extracted with a bias voltage of 10 V and transported to the target chamber. The positrons were then accelerated at 5 keV to a Cu sheet as a target material. Gamma-rays emitted from the target were detected by a Ge gamma-ray detector or a scintillation detector.

Figure 5 shows the gamma-ray spectra from the Ge detector during transporting positrons to the target chamber. A bias voltage was applied to the chopper electrode during the experiment. Figures 5(a) and 5(b) correspond to the spectra with a bias voltage of 0 and 20 V, respectively. A clear annihilation peak at 511 keV was observed at 0V, whereas the annihilation peak decreased to the background level at 20V. This observation means that the positrons emitted from the ^{22}Na source were sufficiently thermalized below 20 eV.

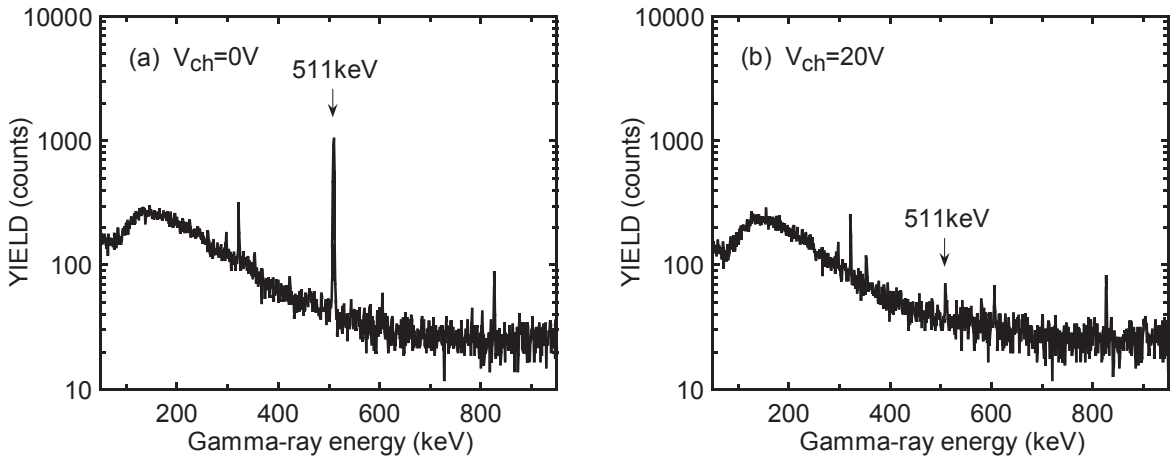

Fig. 5 Gamma-ray spectra measured by changing the chopper voltage from 0V (a) to 20V(b).

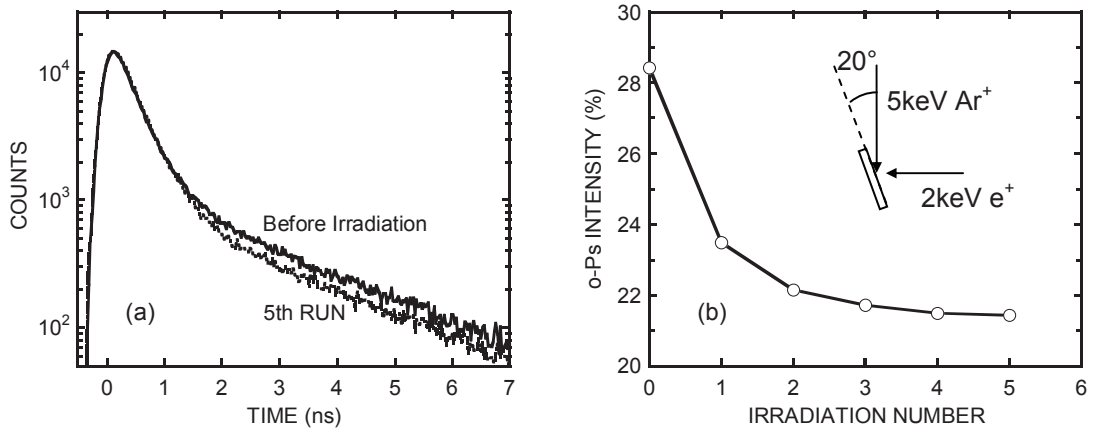

Fig. 6 Preliminary positron lifetime measurements during ion irradiation. (a) Lifetime spectra before the irradiation and during the 5th irradiation. (b) o-Ps intensities during the measurements.

In order to confirm the validity of the simultaneous irradiation method of positron and ion beams, preliminary experiments were performed using the existing positron beamline at the AIST LINAC. An Ar ion gun designed for sputtering was installed on the top of the sample chamber. A polyethylene film was used as a sample and put on a special sample holder with a tilt angle of ~20°. Positron lifetime measurements with a 2 keV positron beam incident from the horizontal direction were performed during the irradiation of a 5 keV Ar^+ beam from the topside. Positron lifetime spectra were measured repeatedly during the ion beam irradiation. Positron annihilation signals of 5×10^5 counts were recorded for each run. The average ion fluence for each run was estimated to be 1×10^{12} cm^{-2}, assuming an ion-beam spot size of 1 cm in diameter. Figure 6(a) shows the lifetime spectra before the irradiation and during the 5th run. The obtained lifetime spectra were decomposed into two lifetime components. The longer lifetime corresponds to the pick-off annihilation of o-Ps. Figure 6(b) shows the o-Ps intensities as a function of run numbers. The decrease in the o-Ps intensity during the ion beam irradiation was clearly monitored. The new positron beamline currently developed has almost the same pulsing electrodes as the existing beamline used for Fig. 6. Thus, this preliminary experiment successfully demonstrated the validity of the irradiation method in the system of this study.

4. Conclusion

A slow-positron beam system for in-situ positron lifetime measurements during ion beam irradiation is currently under development. In this system, slow positrons are generated by a 70 MeV electron beam from a linear accelerator. The positrons are pulsed for lifetime spectroscopy and accelerated up to 30 keV. Ion beams are accelerated up to 150 keV and incident on a target chamber at 45° from the positron beam direction. Beam transport tests were successfully performed by using a weak electron beam from a photocathode and a thermalized positron beam from a radioisotope source. In-situ positron lifetime measurements during ion irradiation were also demonstrated using the existing positron beamline, indicating the validity of the irradiation method.

Acknowledgements

This study was financially supported in part by the Budget for Nuclear Research of the Ministry of Education, Culture, Sports, Science and Technology of Japan, based on screening and counseling by the Atomic Energy

Commission. We would like to thank T. Yoshiie, Q. Xu (Kyoto Univ.), T. Iwai (Tokyo Univ.), Y. Kobayashi and K. Ito (AIST) for their assistance in the early stage of this study.

References

[1] See for example, M. Kiritani, N. Yoshida, H. Takata and Y. Maehara, J. Phys. Soc. Jpn. 38 (1975) 1677.
[2] R.C. Birtcher, J. Mater. Res. 20 (2005) 1654.
[3] J. A. Hinks, Nucl. Instr. and Meth. B267 (2009) 3652.
[4] H. Naramoto, Y. Aoki, S. Yamamoto and H. Abe, Nucl. Instr. and Meth. B127/128 (1997) 599.
[5] W. Möller, W. Fukarek, S. Grigull, O. Kruse and S. Parascandola, Nucl. Instr. and Meth. B136-138 (1998) 1203.
[6] A. Koniger, C. Hammnerl, W. Zander, B. Rauschenbach and B. Stritzker, Rev. Sci. Instrum. 67 (1996) 3961.
[7] T. Iwai, Y. Ito and M. Koshimizu, J. Nucl. Mater. 329-333 (2004) 963.
[8] A. Kinomura, R. Suzuki, T. Ohdaira, N. Oshima, K. Ito, Y. Kobayashi and T. Iwai, J. Phys. Conf. Ser. 262 (2011) 012029.
[9] H. Tsuchida, T. Iwai, M. Awano, M. Kishida, I. Katayama, S.-C. Jeong, H. Ogawa, N. Sakamoto, M. Komatsu and A. Itoh, J. Phys.: Condens. Matter. 19 (2007) 136205.
[10] H. Tsuchida, H. Tanaka, S. Kasai, M. Akiyoshi and A. Itoh, Presentation at the Workshop on Clarification of Materials Irradiation Effects and Improvement of Irradiation Techniques, March 10, 2009, Kumatori-cho, Osaka, Japan.
[11] R. Suzuki, T. Ohdaira and T. Mikado, Radiat. Phys. and Chem. 58 (2000) 603.